www.czasopisma.pan.pl PAN www.journals.pan.pl

ARCHIVES of FOUNDRY ENGINEERING

ISSN (2299-2944)
Volume 2023
Issue 3/2023

22 – 29

10.24425/afe.2023.144311

4/3

Published quarterly as the organ of the Foundry Commission of the Polish Academy of Sciences

Correlation Between K-value, Density Index and Bifilm Index in Determination of Liquid Al Cleanliness

A. Tigli [a, b], **M. Tokatli** [c], **E. Uslu** [c], **M. Colak** [c], **D. Dispinar** [a, d, *]

[a] Istanbul Technical University, Turkey
[b] Sinop University, Turkey
[c] Bayburt University, Turkey
[d] Foseco, Netherlands
* Corresponding author E-mail address: derya.dispinar@gmail.com

Received 20.01.2023; accepted in revised form 20.03.2023; available online 31.07.2023

Abstract

Aluminum alloys are widely used in the industry thanks to its many advantages such as light weight and high strength. The use of this material in the market is increasing day by day with the developing technology. Due to the high energy inputs in the primary production, the use of secondary ingots by recycling from scrap material are more advantageous. However, the liquid metal quality is quite important in the use of secondary aluminum. It is believed that the quality of recycled aluminum is low, for this purpose, many liquid metal cleaning methods and test methods are used in the industry to assess the melt cleanliness level. In this study, it is aimed to examine the liquid metal quality in castings with varying temperature using K mold. A206 alloy was used, and the test parameters were selected as: (i) at 725 °C, 750 °C and 775 °C casting temperatures, (ii) different hydrogen levels. The hydrogen level was adjusted as low, medium and high with degassing, as-cast, and upgassing of the melt, respectively. The liquid metal quality of the cast samples was examined by the K mold technique. When the results were examined, it was determined that metal K values and the number of inclusions were high at the as-cast and up-gas liquid with increasing casting temperatures. It has been understood that the K mold technique is a practical method for the determination of liquid metal quality, if there is no reduced pressure test machine available at the foundry floor.

Keywords: A206 aluminum casting, K mold, Liquid metal cleaning, RPT, Secondary aluminum

1. Introduction

Aluminum alloys are important engineering materials due to their light weight, low density, high corrosion resistance, high electrical and thermal conductivity, high strength and ductility. Therefore, it is widely used in different applications such as automotive, aerospace, defense, aerospace industry, and machinery [1]. It is also known that aluminum alloys are needed more and more every day in the automotive industry due to lowered emission requirements [2].

The raw materials required for aluminum casting are basically supplied in two different ways. The first of these is primary production by extraction of aluminum from ore, and the other from scrap (secondary ingot) through recycling. In the ore production, bauxite ore is mined, and alumina is obtained by the Bayer Process. After this process, pure aluminum is obtained by applying electrolysis process [3]. This method requires high energy input. The amount of energy required during the production of aluminum by recycling from scrap is comparatively low which is around only 5% of the primary production. Secondary aluminum production is important because aluminum is a metal with good recyclability, low energy consumption during remelting etc [4], [5]. The importance of recycling and secondary production is increasing due to limited reserves and bauxite resources that are decreasing day by day. However, the most important problem encountered in the use of secondary aluminum by recycling is the optimization of the liquid metal quality and the need for additional processes to clean the melt [6].

In the production of parts by aluminum alloys casting, the liquid metal quality is negatively affected by possible defects such as Fe-containing intermetallic phases, bifilms, dissolved hydrogen and inclusions [7], [8]. Low liquid metal quality may cause the casting parts to be separated as scrap, as well as adversely affect fluidity and mechanical properties due to the formation of micropores and cracks in the cast parts [9-13]. In order to produce high quality products from secondary aluminum, which has a serious economic value in the industry, it is necessary to increase the quality of the liquid metal. In this context, many liquid metal cleaning processes are developed. Some of them involve the use of flux as lance-assisted degassing, rotary type degassing, electromagnetic degassing, spray degassing, ultrasonic degassing, and vacuum degassing [14-17]. Foundries apply different cleaning methods depending on capacity and production procedure [18].

Various academic studies have been conducted on degassing methods. Ultrasonic degassing for low-pressure die casting was studied by Da Silva [19] and compared with rotary Ar degassing. They reported that ultrasonic degassing was as efficient as Ar degassing in 150 kg furnace resulting with slightly better ductility in 356 alloy. Eskin et al [20] investigated ultrasonic degassing kinetics and compared it to rotary Ar degassing. An AlSpek-H, reduced pressure test (RPT), and 3D X-ray tomography were used to investigate the effects of ultrasonic degassing on porosity formation. They suggested that shorter degassing times can be used by ultrasonic degassing and less dross formation was reported.

Fan et all [21] used high shear device to achieve homogeneous finer microstructure with decreased porosity. Galarraga et al [22] investigated the efficiency of the rotary and ultrasonic degassing system on an AlSi10Mg casting alloy. They used RPT, Archimedes' principal density method. They reported that rotary degassing has higher volumetric efficiency than ultrasonic degassing. In their study, Mostafaei et al [23] examined the effect of rotary degassing parameters, such as degassing time and flow rate, on melt and casting quality. They show that the quality of melt depends on gas flow rate and rotation speed of the lance.

Various test methods are also available to check the assessment of liquid metal cleanliness such as RPT, K-mold technique, thermal analysis method, X-ray method, Tatur test, ultrasonic test, PoDFA method, Qualiflash disk method, Brightimeter technique and electrical resistance method [24-27]. Among these test methods, the most commonly used ones in terms of investment cost, rapid evaluation, and application practicality are known to be RPT and K-mold techniques [28].

The K-mold test method was first applied in 1973 by Sanji Kitaoka (Nippon Light Metal Ltd.) in Japan [29]. The test method is based on the inspection procedure of the fracture surfaces of the cast part. The purpose of the test is to evaluate the macro cleanliness of the aluminum melt before casting. Compared to other liquid metal test methods, the method has advantages such as being economical, easy sampling, rapid evaluation, and sensitivity to inclusions and oxide film [30].

In the K mold technique, after casting, the specimens are removed from the mold and fractured from the notch areas. A macro-scale analysis is performed on the cross-sectional surfaces to detect inclusions. Liquid metal quality is determined by K value as seen in Equation 1.

$$K = s / n \qquad (1)$$

K: the number of inclusions on the fracture surface of a part of the sample,

s: the total number of inclusions found without size-dependent in the fragment,

n: refers to the number of samples examined.

Liquid metal cleanliness can be determined according to the K value. When $K<0.5$, $0.5<K<1.0$, $K>1.0$ are clean, acceptable, and not acceptable respectively [10]. Therefore, when K values are bigger than 1, it means that the liquid metal should be cleaned further.

Gyarmati [31] investigated relation between bifilm and porosity formation in aluminum castings. They used K-mold method, Reduced pressure test (RPT), X-ray computed tomography (CT) in their studies. They observed that the number of pores in RPT sample and Bifilm quantity in K-mold samples were proportional to each other.

Gyarmati et al [32] also investigated the efficiency of rotary degassing system on melt quality of Al-Si alloys by similar techniques. It was reported that wrinkled oxides had covered the surface of the dendrites. These phenomena indicate that porosity formation in aluminum castings was initiated by bifilms (double oxide layers). These observations were compatible with Campbell's theory [33-35] which stated that the bifilms are the main reason for both shrinkage and gas porosity in aluminum.

As mentioned before, the cleanliness of the liquid metal is very important in aluminum castings. In this study, the quality of liquid metal of A206 alloy in different gas content and casting temperatures was investigated by the K-mold technique and RPT (reduced pressure test).

2. Materials and Methods

2.1. Material

In this study, secondary A206 aluminum ingot was used. The chemical composition (% wt.) of the A206 alloy is given in Table 1.

Table 1.
Composition of the A206 aluminum alloys used in the casting experiments

Fe	Si	Cu	Mn	Mg	Zn	Ni	Ti	Al
0.085	0.0121	4.75	0.33	0.36	0.026	0.02	0.00666	rem

2.2. Melting process and casting experiments

Melting operations were carried out in an electric resistance furnace with 10 kW power. A10 type SiC crucible with an 8 kg capacity was used. The melt temperatures were set to 725, 750 and 775 °C. The gas content was set to three levels: as-cast (mid), de-gassed (low), up-gassed (high). For each condition, samples were collected for K-mold and RPT. K-mold was coated with BN and heated to 200°C. The degassing was carried out with nitrogen gas with 5 l/min gas flow rate by using a graphite lance for 10 minutes. For the up-gassing, water vapor was applied to the surface of liquid metal (for 15 minutes) to increase the hydrogen level in the liquid metal. The schematic representation of the casting furnace is given in Fig 1.

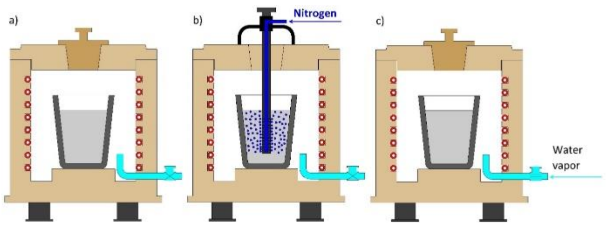

Fig 1. Casting furnace system, (a) as-cast, (b) degassed, (c) upgassed

K-mold is 240 mm long, 36 mm wide, and 6 mm thick. There are notches in the sample, as seen in Fig. 2. After the samples were collected by ladle and poured into the mould, the inclusions on the fracture surfaces of the 5 pieces obtained from the sample were examined by the macro examination method. In order to examine the samples, high-resolution photographs of the fractured surfaces of the samples should be taken. Photographs of the sample fracture surfaces were taken with a Sony A7R3 camera with 42.4 MP resolution. Inclusion counting was performed from the obtained images with the image analysis method and K values were recorded according to Equation 1. Detailed information about K-mold method and K values can be found in the following articles [36, 37].

Reduced pressure test (RPT) was carried out at 100 mbar. The density of the samples was measured by Archimedes principle and the bifilm index was measured from the cross-section of samples. The following articles provide detailed information about RPT sample preparation and bifilm index [38], [39].

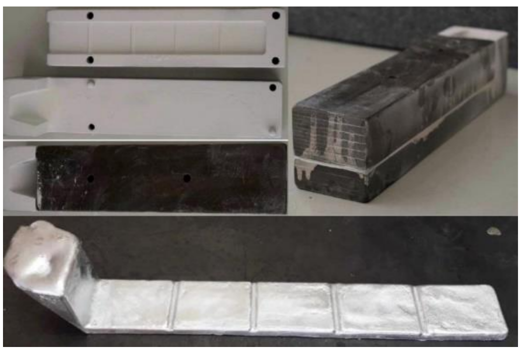

Fig. 2. K-mold and a representative cast sample

3. Results and Discussion

The castings were completed at three different casting conditions (de-gassing, as-cast, and up-gassing) and at three different casting temperatures (725, 750, and 775 °C). The cast samples were fractured into 5 pieces by using the notches to create fracture surfaces. High-resolution photographs were taken of the fractured surfaces of these five stacked pieces. Images of the K-mold samples are given in Figure 3. The image of these fracture surfaces of K mold test samples was examined by using macro examination methods.

It can be seen in Figure 3 that the inclusions and defects can be clearly detected in macro images. The inclusion and defects on the fractured surfaces are counted without any discrimination in 5 pieces of K-mold sample for each condition. During this procedure, the total number of inclusions and defects is recorded regardless of the defect size.

It was observed that there was an increase in inclusion with the increase in temperature in all experimental conditions (different gassing levels). It is interesting to note that the size of defects was decreasing while the number of defects was increasing with increased temperature. Furthermore, k-mold samples with the up-gassed condition revealed the highest number of defects (K values). On the other hand, in the casting with the degassed conditions, the inclusions on the fracture surface of K-mold samples displayed the lowest K values (fewer inclusions).

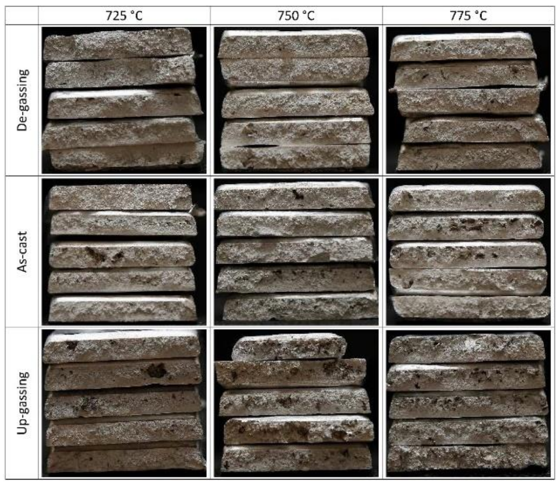

Fig. 3. K-mold samples fracture surfaces on different conditions (de-gassing, as-cast and up-gassing) and 725, 750 and 775 °C casting temperatures

Table 2 represents the total number of defects and K values for each casting condition (gas levels and casting temperatures). The number of inclusions shows the total number of inclusion and defects counted on the surface of all 5 parts of the K-mold sample. The number of K mold parts represents the investigated fractured surface for each casting condition (from one K-mold sample). Therefore, Table 2 is basically a numerical representation of Figure 3. K-values are calculated by dividing the number of mold parts by the number of inclusions (Equation 1).

Table 2.
Calculated K values, the total number of inclusions at 5 fractured surfaces of cast samples at three different casting temperatures and gassing levels (As-cast, Up-gassing, and De-gassing) conditions

Casting	Temperature (°C)	Number of inclusions	Number of K mold parts	K value
As-cast	725	14	5	2.80
As-cast	750	17	5	3.40
As-cast	775	23	5	4.60
Upgassed	725	18	5	3.60
Upgassed	750	22	5	4.40
Upgassed	775	24	5	4.80
Degassed	725	4	5	0.80
Degassed	750	5	5	1.00
Degassed	775	7	5	1.40

It can be seen in Figure 4 that K-value was increased with the increase in the casting temperature in all conditions. The degassed condition has the lowest K-values around 1 while as-cast and up-gassing conditions have similar and highest K-values around 3-5. The studies about liquid metal quality with the K mold test method suggest the use of K values lower than 1 for high liquid metal cleanliness. In degassed castings, it is seen that the liquid metal quality is at acceptable levels below 1. This confirms that the degassing process was efficiently carried out and melt was cleaned from defects. When the test results are examined, it is understood that cleaning should be done because the K values are above 1.00 in all of the as-cast samples [36]. In 775 °C degassing trials, the K value was 1.40. Therefore, it suggests that the liquid metal requires further treatment. Either degassing time or flow rate of nitrogen gas need to be optimized for castings at 775 °C in order to achieve the required high-quality melt cleanliness levels.

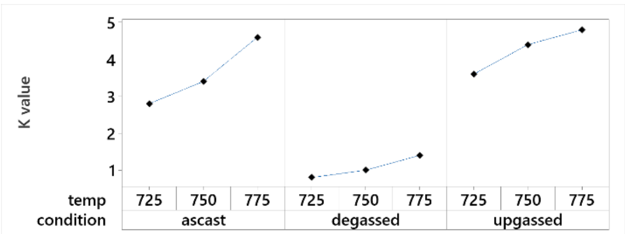

Fig. 4. K-value change by casting temperature (725, 750 and 775 °C) and casting conditions (As-cast, up-gassing and de-gassing)

As seen in Figures 3 and 4, the increased K-value in up-gassed castings can be attributed to the increased oxidation rate in aluminum with increased temperature. The transformation of amorphous alumina to crystalline γ-Al_2O_3 is enhanced due to the fast migration of oxygen through the oxide-metal interface. During this transformation, the volume of the oxide decreases which is known as breakaway oxidation. Thus, a single large oxide now tears into fine and smaller ones. Additionally, depending on the Mg content of the alloy, $MgAl_2O_4$ spinel oxides may form which also has the tendency to form breakaway oxidation. Based on data from Table 2, the change in the number of defects with temperature was plotted. As seen in Figure 5, as the temperature increased, the number of defects increase almost linearly. Furthermore, the number of defects also increases depending on casting conditions at the same casting temperature. For example, K-mold samples have 4, 14, and 18 defects for de-gassing, as-cast, and up-gassing casting at 725 °C, respectively.

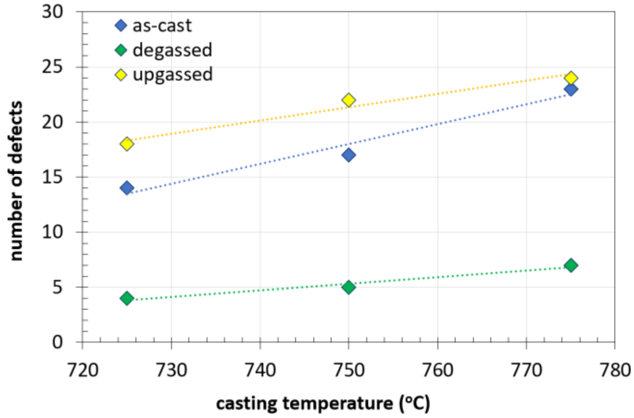

Fig. 5. Change in number of defects by casting temperature (725, 750 and 775 °C) and casting conditions (As-cast, up-gassing and de-gassing)

Figures 6, 7, and 8 represent the SEM (Scanning electron microscopy) Images of K-mold samples at the different casting conditions (different gassing levels). Figure 6 shows the SEM images of the fractured surfaces of K-mold samples at as-cast conditions. These figures displayed those oxides are observed on the surface of the fractured surfaces. These oxides have a geometry that resembles a crumpled paper and can be clearly seen in the fracture surface of samples (Figure 6 a-d). This crumpled geometry is an indication of turbulent motion of the oxide either within the melt or that could occur during filling. These were mainly observed in the as-cast condition.

Figure 7 shows the SEM images of fractured K-mold samples at up-gassing conditions. There was also the flat and rigid type of thick old oxides on the fracture surface. Their size changed from 300 to 600 µm as seen in Figure 7 a-d. These flat and rigid type oxides were mainly observed in the up-gassed casting condition.

Figure 8 shows the porosity images in SEM photos at all casting conditions. Some pores on the fracture surface were associated with dendrites clearly seen on the fracture surface (Figure 8). One particular defect was quite interesting where an oxide was covering the dendrite as seen in Figure 8-c. As seen in Figure 8-d, most of the fracture surface was typical brittle morphology with negligible amount of porosity and oxides. It has a microscopically rough surface more typical of nitride bifilms resulting from the nitrogen degassing. The nitrogen degassing would have floated out all the original macroscopic or mesoscopic alumina bifilms but generated huge numbers of microscopic bifilms from the bursting of the nitrogen bubbles at the surface (the two halves of the opposite surfaces of each bubble coming together to make a bifilm), therefore producing a huge population of fine bifilms (probably nitride bifilms). On the other hand, in the degassed castings, no particular defect was detected.

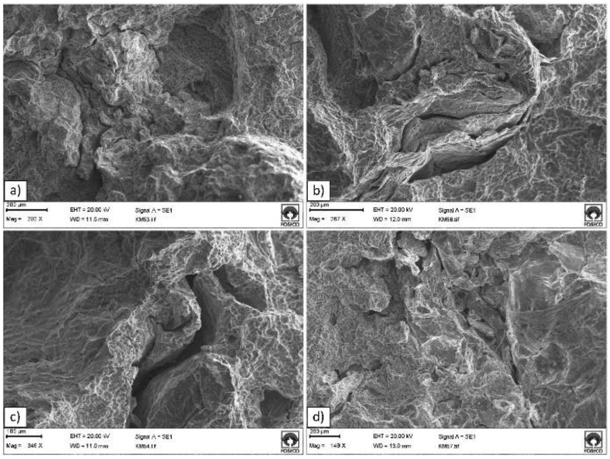
Fig. 6. SEM images of crumpled oxides on the fracture surface of as-cast samples

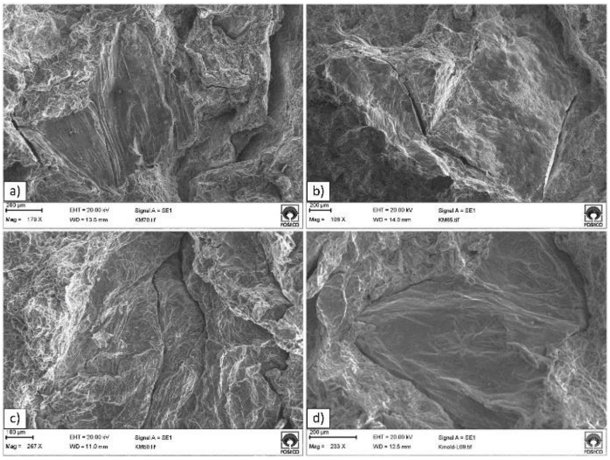
Fig. 7. SEM images of thick and rigid old oxides on the fracture surface on the up-gassed samples

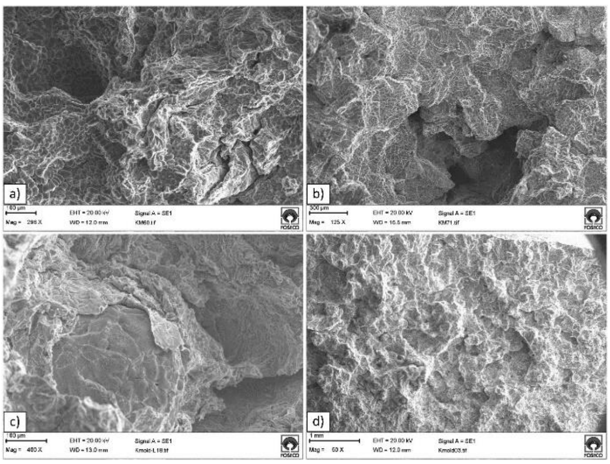
Fig. 8. SEM images of various types of porosity observed on the fracture surface of K-mold samples

In order to assess the effect of melt treatment on K-mold tests, the change in K values (ΔK) is calculated using Equation 2 given below.

$$\Delta K = [(K2 - K1) / K1] \times 100 \qquad (2)$$

Figure 9 represents the change in K values (ΔK) based on the as-cast samples for all casting temperatures. In de-gassing casting, approximately 70% decrease is observed based on the as-casting samples for all temperatures. On the other hand, up to 25% increase in K-values for the up-gassed condition.

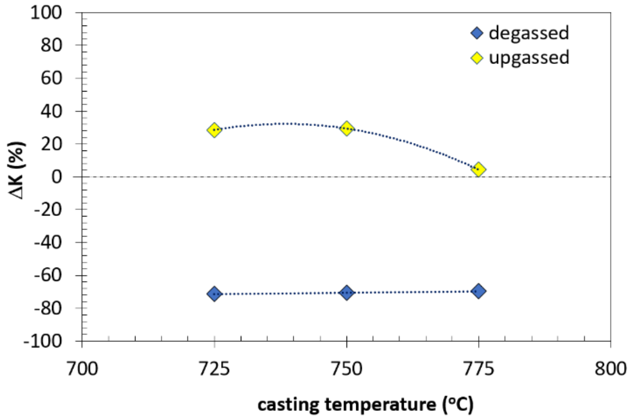

Fig. 9. Change in K-values by temperature and melt treatment

According to the density of RPT samples, it can be seen in Fig. 10 that the degassed condition had the highest density values ranging from 2.73-2.78 g/cm^3 while the upgassed condition had the lowest density values. It is interesting to observe that the density was increasing with increased temperature for as-cast and degassed conditions while the density was in decreasing trend for the upgassed melt. On Fig. 11, the change in bifilm index with temperature and casting conditions are given. It can be seen that the bifilm index was decreasing with increased temperature for as-cast and degassed condition while a significant increase was observed for the upgassed condition.

Figure 10 displays the density of RPT samples which is cast at different gassed level and casting temperatures. According to the density of RPT samples, it can be seen in Figure 10 that the de-gassed condition had the highest density values ranging from 2.73-2.78 g/cm^3. On the other hand, the up-gassed RPT samples had the lowest density values ranging from 2.61-2.73 g/cm^3. It is interesting to observe that the density was increasing with increased temperature for as-cast and degassed conditions while the density was in decreasing trend for the up-gassed RPT samples. The decrease in density might be explained by formed porosity due to high gassing levels during up-gassing of samples under reduced pressure casting.

The change in bifilm index with temperature and casting conditions are given in Figure 11. It can be seen that the bifilm index was decreasing with increased temperature for as-cast and degassed conditions. on the other hand, a significant increase was observed at elevated temperatures for the up-gassed condition. The bifilm indexes are approximately 6, 25 and 72 mm at 725, 750 and 775 °C casting temperatures, respectively. This increase can be explained by the formation of new bifilms during the steam-applying process. These bifilms are unfurled under reduced pressure and being visible. Therefore, new porosities are formed and expended at A206 RPT samples. These new formed porosities might be main reason at the decrease of density with increasing casting temperature at up-gassed RPT samples.

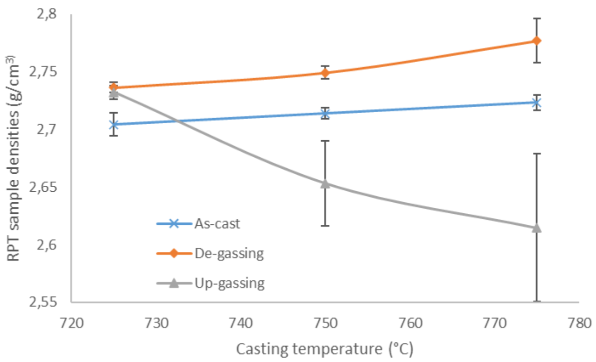

Fig. 10. Change in density of RPT samples with casting temperature and different casting conditions (as-cast, de-gassing and up-gassing)

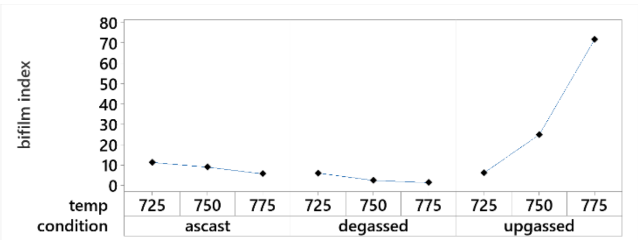

Fig. 11. Change in bifilm index at different casting conditions and temperatures

The correlation between bifilm index, density and K-values were also evaluated. The results are summarized in Fig. 12 and Fig. 13. Both values (bifilm index and density of RPT) appear to have an exponential relationship with K values. The scatter of density results vs K-values is wider compared to bifilm index. When K-value is low, density is high and bifilm index is low. However, at high K-values (between 4-5), both the density and bifilm index values scatter significantly which indicates that sensitivity of the tests with regard to the melt cleanliness varies dramatically. Therefore, it can be concluded that when the melt cleanliness is high (i.e. bifilm index lower than 20 mm), K values of up to 3 could be acceptable. On the other hand, the highest cleanliness was achieved when bifilm index was lower than 10 mm which corresponded to K values of lower than 1,3. As a result, the best conditions of melt cleanliness and defect-free castings could be achieved when bifilm index is lower than 10 and K mould is lower than 1. Erzi et al [40] had shown that density index could be misleading to assess melt cleanliness level due to the fact that not all pores are always round, instead, occasionally they can be flat or crack-like shapes. In this way, the density will be high, but a large defect would be present in the melt. As seen in Fig. 13, the lowest K-value (< 1) is achieved when density is high and bifilm index is lower than 10 mm.

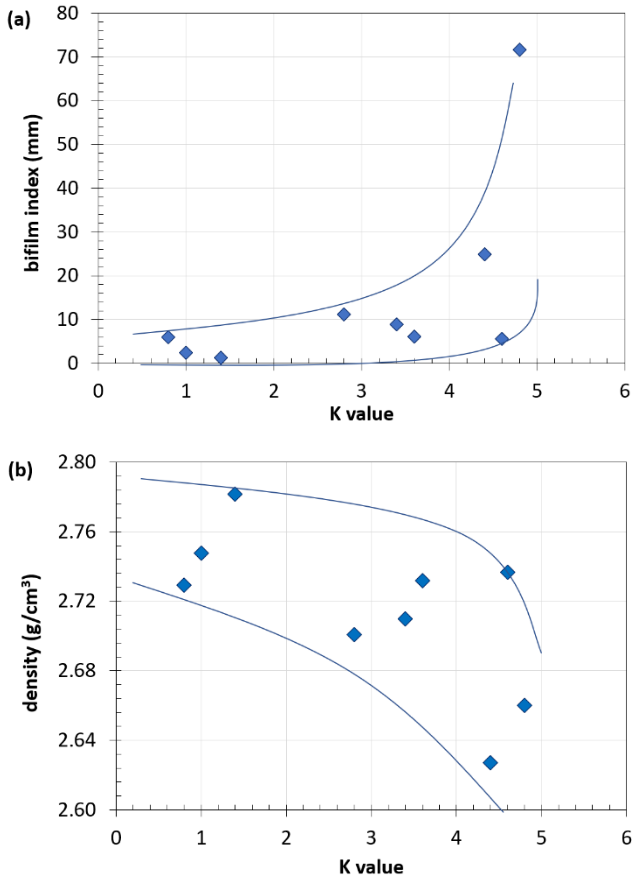

Fig. 12. Change in K-values with (a) bifilm index, (b) density of RPT samples

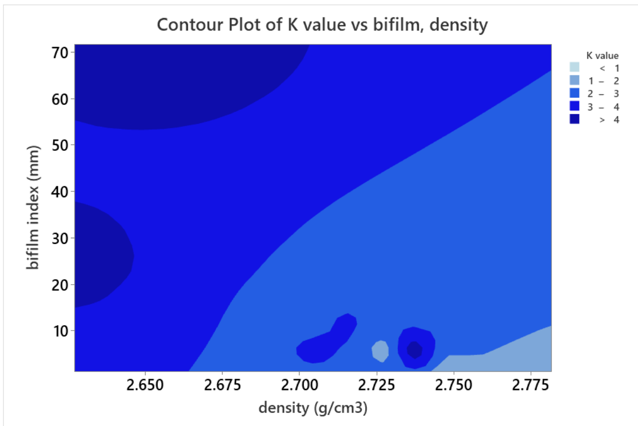

Fig. 13. Contour map of bifilm index, density of RPT and K-values

4. Conclusions

In this study, an investigation was carried out on the assessment of the liquid metal quality with the K-mold and RPT technique in the casting of A206 aluminum alloy at varying temperatures and different gas levels. In conclusion:

Casting temperature is important for liquid metal quality. The number of inclusions in a casting product increases as temperatures increases. This is attributed to the breakaway oxidation which results in smaller and higher number of oxide defects in the melt. Therefore, melt cleanliness level is adversely affected by increased melt temperature.

Degassing decreases the number of inclusions in the melt and melt cleanliness increases. Without degassing, the K values in the castings are high at all temperatures. The degassing process is therefore necessary for these alloys in order to have good quality castings.

In the degassing castings, the K value is at an acceptable level (below 1.0) at temperatures of 725 °C and 750 °C. However, with the increase in temperature, the K value increased to 1.40 in the casting made at 775 °C. In order to achieve K values lower than 1 (i.e. good quality melt), bifilm index need to be lower than 10 mm.

Based on all this information, it has been concluded that the best conditions of melt cleanliness and defect-free castings could be achieved when bifilm index is lower than 10 and K value is lower than 1. For foundries who does not use or have RPT machine, simple K-mold could be an alternative practical solution.

References

[1] Brooks, C.R. (1982). *Heat treatment, structure, and properties of nonferr ous alloys*.

[2] Chen, W.-F., Lui, E.M. (2005). *Handbook of structural engineering*. CRC press. https://doi.org/10.1201/9781420039931.

[3] Balomenos, E., Panias, D. & Paspaliaris, I. (2011). Energy and exergy analysis of the primary aluminum production processes: A review on current and future sustainability. *Mineral Processing & Extractive Metallurgy Review*. 32(2), 69-89. https://doi.org/10.1080/08827508.2010.530721.

[4] Lin, R., Liu, B., Zhang, J. & Zhang, S. (2022). Microstructure evolution and properties of 7075 aluminum alloy recycled from scrap aircraft aluminum alloys. *Journal of Materials Research and Technology*. 19, 354-367. https://doi.org/10.1016/j.jmrt.2022.05.011.

[5] Odusote, J.K. & Ajayi, P.A. (2016). Mechanical properties and microstructure of recycled aluminum cast with zinc and copper additions. *International Journal of Metalcasting*. 10(4), 483-490. https://doi.org/10.1007/s40962-016-0060-4.

[6] Sigworth, G. (2011). Understanding quality in aluminum castings. *International Journal of Metalcasting*, 5, 7-22. https://doi.org/10.1007/BF03355504.

[7] Scampone, G., Pirovano, R., Mascetti, S. & Timelli, G. (2021). Experimental and numerical investigations of oxide-related defects in Al alloy gravity die castings. *The International Journal of Advanced Manufacturing Technology*. 117(5), 1765-1780. https://doi.org/10.1007/s00170-021-07680-5.

[8] Fiorese, E., Bonollo, F., Timelli, G., Arnberg, L. & Gariboldi, E. (2015). New classification of defects and imperfections for aluminum alloy castings. *International Journal of Metalcasting*. 9(1), 55-66. https://doi.org/10.1007/BF03355602.

[9] Kaufman, J.G., Rooy, E.L. (2004). *Aluminum alloy castings: Properties, processes, and applications*. Asm International.

[10] Chiesa, F. & Regimbal, P. (2001). Distinguishing Microporosity From Macroshrinkage When Modeling Solidification of A 356 Castings. *Transactions of the American Foundry Society and the One Hundred Fifth Annual Castings Congress*. 1-11.

[11] Dispinar, D. & Campbell, J. (2011). Porosity, hydrogen and bifilm content in Al alloy castings. *Materials Science and Engineering: A*. 528(10-11), 3860-3865. https://doi.org/10.1016/j.msea.2011.01.084.

[12] Singh, D. & Mitchel, D. (2001). Analysis of metal quality in a low pressure permanent mold foundry. *Transactions of the American Foundry Society and the One Hundred Fifth Annual Castings Congress*. 1-13.

[13] Kong, D., Sun, D.-Z., Yang, B., Qiao, H., Wei, C., Lang, Y., Song, H. & Gao, J. (2023). Characterization and modeling of damage behavior of a casting aluminum wheel considering inhomogeneity of microstructure and microdefects. *Engineering Failure Analysis*. 145, 107018, 1-25. DOI:10.1016/j.engfailanal.2022.107018.

[14] Tan, E., Tarakcılar, A., Dıspınar, D., Colak, M. & Kayıkcı, R. (2011). Reproducibility of reduced pressure test results in testing of liquid aluminum gas levels. In 6th International Advanced Technologies Symposium (IATS'11), 16-18 May 2011 (pp.18). Elazig, Turkey.

[15] Çolak, M., Kayikci, R. & Dispinar, D. (2016). Melt cleanliness comparison of chlorine fluxing and Ar degassing of secondary Al-4Cu. *Metallurgical and Materials Transactions B*, 47, 2705-2709. DOI:10.1007/s11663-016-0745-3.

[16] Lazaro-Nebreda, J., Patel, J.B., Lordan, E., Zhang, Y., Karakulak, E., Al-Helal, K., Scamans, G.M. & Fan, Z. (2022). Degassing of aluminum alloy melts by high shear melt conditioning technology: an overview. *Metals*, 12(10), 1772, 1-21. https://doi.org/10.3390/met12101772.

[17] Nasresfahani, M.R. & Niroumand, B. (2020). Effect of degassing on hot tearing tendency of A206 aluminum cast alloy. *International Journal of Metalcasting*. 14(2), 538-546. https://doi.org/10.1007/s40962-019-00378-1.

[18] Reddy, B.M. & Nallusamy, T. (2021). Degassing of aluminum metals and its alloys in non-ferrous foundry. *Advances in Materials Research*. 5, 637–644. https://doi.org/10.1007/978-981-15-8319-3_63.

[19] da Silva, M., Rebolledo, L., Pabel, T., Petkov, T., Planta, X., Tort, J. & Eskin, D. (2015). Evaluation of effect of ultrasonic degassing on components produced by low pressure die casting. *International Journal of Cast Metals Research*. 28(4), 193-200. https://doi.org/10.1179/ 1743133614Y.0000000141.

[20] Eskin, D., Alba-Baena, N., Pabel, T. & da Silva, M. (2015). Ultrasonic degassing of aluminium alloys: Basic studies and practical implementation. *Materials Science and Technology*. 31(1), 79-84. DOI:10.1179/1743284714Y.0000000587.

[21] Fan, Z.Y., Zuo, Y.B. & Jiang, B. (2011). A new technology for treating liquid metals with intensive melt shearing. *Materials Science Forum*. 690, 141-144. https://doi.org/10.4028/www.scientific.net/MSF.690.141.

[22] Galarraga, H., García de Cortázar, M., Arregi, E., Artola, A., Oncala, J. & Merchán-Zubieta, M. (2020). Gas blowing ultrasonic aluminium degassing assessment with the reduced pressure test (RPT) method. *Archives of Foundry Engineering*. 20(2), 111-117. DOI:10.24425/afe.2020.131312.

[23] Mostafaei, M., Ghobadi, M., Eisaabadi B,G., Uludağ, M. & Tiryakioğlu, M. (2016). Evaluation of the effects of rotary degassing process variables on the quality of A357 aluminum alloy castings. *Metallurgical and Materials Transactions B*, 47, 3469-3475. DOI:10.1007/s11663-016-0786-7.

[24] Lashkari, O., Yao, L., Cockcroft, S. & Maijer, D. (2009). X-ray microtomographic characterization of porosity in aluminum alloy A356. *Metallurgical and Materials Transactions A*. 40(4), 991-999. DOI:10.1007/s11661-008-9778-9.

[25] Brůna, M. & Sládek, A. (2011). Hydrogen analysis and effect of filtration on final quality of castings from aluminium alloy AlSi7Mg0,3. *Archives of Foundry Engineering*. 11(spec.1), 5-10. ISSN (1897-3310).

[26] Habibi, N., Samuel, A., Samuel, F., Rochette, P. & Paquin, D. (2004). Effect of grain refining and Sr modification on Prefil measurement sensitivity in 356 alloys using electron probe microanalysis technique. *International Journal of Cast Metals Research*. 17(2), 79-87. https://doi.org/10.1179/136404604225014837.

[27] Paradis, M., Samuel, A., Doty, H. & Samuel, F. (2018). Inclusion measurement and identification in Mg-based alloys: Application of the brightimeter technique. *International Journal of Metalcasting*. 12(7), 2-19. https://doi.org/10.1007/s40962-016-0130-7.

[28] Haberl, K., Schumacher, P., Geier, G. & Stauder, B. (2009). Characterization of the melt quality and impurity content of an LM25 alloy. *Metallurgical and Materials Transactions B*. 40(6), 812-821. DOI:10.1007/s11663-009-9282-7.

[29] Hudson, S.W. & Apelian, D. (2016). Inclusion detection in molten aluminum: Current art and new avenues for in situ analysis. *International Journal of Metalcasting*. 10, 289-305. https://doi.org/10.1007/s40962-016-0030-x.

[30] Djurdjević, M.B., Odanović, Z. & Pavlović-Krstić, J. (2010). Melt quality control at aluminum casting plants. *Metallurgical & Materials Engineering*. 16(1), 63-76.

[31] Gyarmati, G., Fegyverneki, G., Mende, T. & Tokár, M. (2019). Characterization of the double oxide film content of liquid aluminum alloys by computed tomography. *Materials Characterization*. 157, 109925. DOI:10.1016/j.matchar.2019.109925.

[32] Gyarmati, G., Fegyverneki, G., Tokár, M. & Mende, T. (2021). The effects of rotary degassing treatments on the melt quality of an Al–Si casting alloy. *International Journal of Metalcasting*. 15(1), 141-151. https://doi.org/10.1007/s40962-020-00428-z.

[33] Campbell, J. (2015). *Complete casting handbook: Metal casting processes, metallurgy, techniques and design*. UK: Butterworth-Heinemann.

[34] Dispinar, D. & Campbell, J. (2004a). Critical assessment of reduced pressure test. Part 1: Porosity phenomena. *International Journal of Cast Metals Research*. 17(5), 280-286. DOI:10.1179/136404604225020696.

[35] Dispinar, D. & Campbell, J. (2004). Critical assessment of reduced pressure test. Part 2: Quantification. *International Journal of Cast Metals Research*. 17(5), 287-294. DOI:10.1179/136404604225020704.

[36] Gyarmati, G., Vincze, F., Fegyverneki, G., Kéri, Z., Mende, T. & Molnár, D. (2022). The effect of rotary degassing treatments with different purging gases on the double oxide- and nitride film content of liquid aluminum alloys. *Metallurgical and Materials Transactions B*. 53(2), 1244-1257. https://doi.org/10.1007/s11663-021-02414-0.

[37] Máté, M., Tokár, M., Fegyverneki, G. & Gyarmati, G. (2020). The Comparative Analysis of the Inclusion Removal Efficiency of Different Fluxes. *Archives of Foundry Engineering*. 20(2), 53-58. DOI: 10.24425/afe.2020.131302.

[38] Dispinar, D. & Campbell, J. (2014). Reduced pressure test (RPT) for bifilm assessment. Shape Casting: 5th International Symposium (pp. 243-251). Springer, Cham.

[39] Yüksel, Ç., Dışpınar, D. & Çiğdem, M. (2022). An analytical approach for the correlation between bifilm index and tensile properties of alsi7mg0. 3 (a356) aluminum alloy cleaned via rotary degassing and different fluxes. *International Journal of Metalcasting*. 9(1), 1-13. DOI:10.1007/s40962-022-00882-x.

[40] Erzi, E., Gürsoy, Ö., Yüksel, Ç., Colak, M. & Dispinar, D. (2019). Determination of acceptable quality limit for casting of A356 aluminium alloy: Supplier's quality index (SQI). *Metals*. 9(9), 957, 1-14. https://doi.org/10.3390/met9090957.